Chemical Geology 377 (2014) 12–19

Contents lists available at ScienceDirect

Chemical Geology

journal homepage: www.elsevier.com/locate/chemgeo

Climate sensitivity and parameter coherency in annually resolved $\delta^{13}C$ and $\delta^{18}O$ from *Pinus uncinata* tree-ring data in the Spanish Pyrenees

Oliver Konter [a,*], Steffen Holzkämper [a,b], Gerhard Helle [c], Ulf Büntgen [d], Matthias Saurer [e], Jan Esper [a]

[a] Department of Geography, Johannes Gutenberg University, Becherweg 21, 55099 Mainz, Germany
[b] Department of Physical Geography and Quaternary Geology, Stockholm University, 10691 Stockholm, Sweden
[c] German Centre for Geosciences-GFZ, Section 5.2 Climate Dynamics and Landscape Evolution, Potsdam, Germany
[d] Swiss Federal Research Institute for Forest Snow and Landscape (WSL), 8903 Birmensdorf Switzerland
[e] Paul Scherrer Institut, Villigen PSI, Switzerland

ARTICLE INFO

Article history:
Received 19 December 2013
Received in revised form 24 March 2014
Accepted 31 March 2014
Available online 12 April 2014

Editor: David R. Hilton

Keywords:
Tree-rings
Stable isotopes
Climate signals
Calibration
Mediterranean

ABSTRACT

We explore the 20th century climate sensitivity of annually resolved carbon and oxygen isotope ratios in five *Pinus uncinata* individuals from the upper treeline in ~2400 m asl of the Spanish Pyrenees. Time series of $\delta^{13}C$ and $\delta^{18}O$ are calibrated against temperature, precipitation, and drought indices over the period 1901–2009. Negative correlations of $\delta^{13}C$ with summer precipitation and drought indices, as well as positive correlations with summer temperatures, confirm previous evidence from similar habitats in the Pyrenees. In contrast to this summer climate signal in the carbon isotopes, the $\delta^{18}O$ record reveals mainly negative correlations with spring precipitation and drought. We explore the coherence between $\delta^{13}C$ and $\delta^{18}O$ time series derived from individual trees and assess the influence of widely applied $\delta^{13}C$ correction procedures on the climate signal strength. Spatial correlation patterns and decomposition of the time series into high- and low-frequency components are used to develop a calibration setup for carbon and oxygen isotope ratios, which will improve long-term climate reconstructions in a region, where classical tree-ring width and density data are limited.

1. Introduction

The influence of temperature on the formation of tree-ring width (TRW) and maximum latewood density (MXD) is well known towards altitudinal and latitudinal treelines, where annually resolved measurements from living trees and relict material allow millennium-long reconstructions to be developed (Büntgen et al., 2008, 2011; Esper et al., 2012). Dendroclimatological studies in the European Mediterranean region reveal temperature-induced growth variations at high-elevation treeline sites (Gutiérrez, 1991; Camarero et al., 1998; Tardif et al., 2003), with MXD generally providing more reliable results in comparison to a reduced sensitivity in TRW (Büntgen et al., 2008, 2010, 2012).

Stable isotope ratios preserved in xylem cells contain information on past environmental conditions and became an important proxy in paleoclimate studies (Helle and Schleser, 2004; Treydte et al., 2007; Planells et al., 2009; Schollän et al., 2013a). However, the climate–isotope relationships for trees growing in high elevation Mediterranean environments are much less explored than in the European Alps, arid regions in the US, or sites in the northern high latitudes, for example (McCarroll and Loader, 2004; Heinrich et al., 2013). The $^{13}C/^{12}C$ ratio of pine trees from different sites in the Spanish Pyrenees revealed positive correlations with June–October temperatures and negative correlations with June–July precipitation (Andreu et al., 2008; Dorado-Liñán et al., 2011b), but the associations are relatively weak compared to evidence from other regions (Dorado-Liñán et al., 2011a).

Dorado-Liñán et al. (2011a) also demonstrated that calibration studies based on pooled isotope time series (that is the combination of wood samples before isotopic analysis) may be biased by non-climatic low-frequency trends. Other work revealed such limitations to be particularly significant, if the number of pooled trees is <5 (Konter et al., 2013).

We here address these issues, and present 20th century, annually resolved, time series of individually measured $\delta^{13}C$ and $\delta^{18}O$ from five *Pinus uncinata* trees from high elevation environments in the Spanish Pyrenees. The measurement series are used to explore the coherency among trees, and to assess their common climatic signal. $\delta^{13}C$ and $\delta^{18}O$ climate signals are evaluated by using instrumental temperature, precipitation and drought data to achieve a deeper understanding of the drivers of tree's isotope fractionation in high elevation environments. Larger scale spatial patterns of climate as well as the effects of $\delta^{13}C$ correction procedures are assessed to evaluate the utilization of tree-ring stable isotope data for reconstruction purposes.

* Corresponding author. Tel.: +49 6131 3922769; fax: +49 6131 39 24735.
E-mail address: o.konter@geo.uni-mainz.de (O. Konter).

http://dx.doi.org/10.1016/j.chemgeo.2014.03.021
0009-2541/

2. Material and methods

2.1. Study site and sample design

The sampling site is situated at ~2400 m asl near Lake Gerber at the northern border of the 'D'Aigüestortes Estany de Sant Maurici National Park' in the Spanish central Pyrenees, west of Andorra (Fig. 1). The prevailing tree species is *P. uncinata*, which aggregates as a shade-intolerant conifer in an open forest ecotone (Camarero et al., 1998). Tree heights vary between 3 and 6 m, and stem circumference at breast height ranges from 0.80 to 3.38 m. The poorly developed soils accumulate in shallow basins and can be identified as skeletal leptosols with no access to ground water (Esper et al., 2010). Between-tree distances vary from 2 to 12 m and the canopy is sparse (about 10%). Annual mean temperature fluctuates around ~4 °C, with maxima in July (~13 °C) and minima in January (~−3 °C) (Büntgen et al., 2008). Monthly precipitation totals (mean annual sum at ~1200 mm) are highest in May (12%) and lowest in July (~6%). Since soils are poorly developed at the sampling site, only a small amount of snowmelt is stored in reservoirs accessible to the trees.

A total of 23 *P. uncinata* trees, growing under similar ecological and climatological conditions, were sampled for initial TRW measurements. Four cores per tree were extracted in a radial configuration at breast height, two parallel and two perpendicular to the slope.

2.2. Stable isotope ratio measurements

For stable isotope measurements, a subset of five trees was selected and each tree-ring from 1901 to 2009 dissected using a scalpel (Leavitt and Long, 1984). Two cores per tree were used and combined to develop five annually resolved wholewood time series spanning the 1901–2009 period. The α-cellulose was extracted from the wholewood samples following procedures detailed in Wieloch et al. (2011). The α-cellulose samples were homogenized by using an ultrasonic device (Laumer et al., 2009), freeze dried prior to analyzing (1) $^{13}C/^{12}C$ ratios using an IsoPrime Isotope Ratio Mass Spectrometer (IRMS) with an interfaced elemental analyzer, and (2) $^{18}O/^{16}O$ ratios using a TC/EA pyrolysis furnace (Thermo Finnigan) coupled online to a Delta V Advantage IRMS. Both devices were operated in continuous flow mode, allowing combusting (carbon) or pyrolizing (oxygen), purifying and transporting the sample on a continuous carrier gas flow at the GFZ in Potsdam. The isotope ratios are expressed in the conventional δ notation and in parts per thousand (‰), relative to the VPDB (Vienna Pee Dee Belemnite) standard for carbon ($\delta^{13}C$) and the VSMOW (Vienna Standard Mean Ocean Water) standard for oxygen ($\delta^{18}O$) (Craig, 1957). Sample replication resulted in a reproducibility of ±0.1‰ for $\delta^{13}C$ and ±0.25‰ for $\delta^{18}O$.

2.3. Time series analyses and corrections

All tree-rings were crossdated and assigned to calendar years, starting with the most recent, fully developed increment in 2009 (trees were sampled in summer 2010). TRW was measured with an accuracy of 0.01 mm using a LinTab measurement device and TSAP software (Rinn, 2007). TRW crossdating was verified by using COFECHA (Holmes, 1983), and different detrending methods (Regional Curve Standardization RCS, 100-year spline) applied using the ARSTAN program (Cook, 1985; Esper et al., 2003).

2.3.1. Tree-ring carbon isotopes

Photosynthetic discrimination of $^{13}CO_2$ against $^{12}CO_2$ is related to the ratio of leaf internal to external CO_2 partial pressure (C_i/C_a), jointly controlled by the stomatal conductance and rate of CO_2 assimilation (Farquhar et al., 1982). Since changes in the atmospheric carbon isotopic source signal are reflected in the tree-ring cellulose, these trends need to be removed in climate studies (Farquhar et al., 1982; Treydte et al., 2009). Accordingly, all tree-ring $\delta^{13}C$ values were corrected to account for the depletion of ^{13}C in the atmosphere's CO_2, due to the burning of fossil fuels and deforestation since ~AD 1850, and resulting values termed $\delta^{13}C_{atm}$.

Exposure to increasing atmospheric CO_2 also leads to changes in internal CO_2 concentrations of the needles, resulting in adaptations of stomatal conductance, water-use-efficiency, and photosynthetic assimilation rate (Farquhar et al., 1982). These processes require consideration before assessing climate–isotope relationships (McCarrol et al., 2009; Treydte et al., 2009; Schubert and Jahren, 2012), and are here corrected considering fixed amounts of isotope fractionation per unit CO_2 increase, following procedures detailed by Feng and Epstein (1995) based on oak tree greenhouse studies, and Kürschner (1996) based on juniper, pine and oak studies in SW-USA and Egypt. Application of the Feng and Epstein (1995) correction alters the $\delta^{13}C_{atm}$ time series by a factor of 0.02‰ per ppm CO_2 change (resulting time series termed $\delta^{13}C_{FE}$), which is quite sizeable compared to the Kürschner (1996) correction of 0.0073/ppm CO_2 (hereafter $\delta^{13}C_K$). These

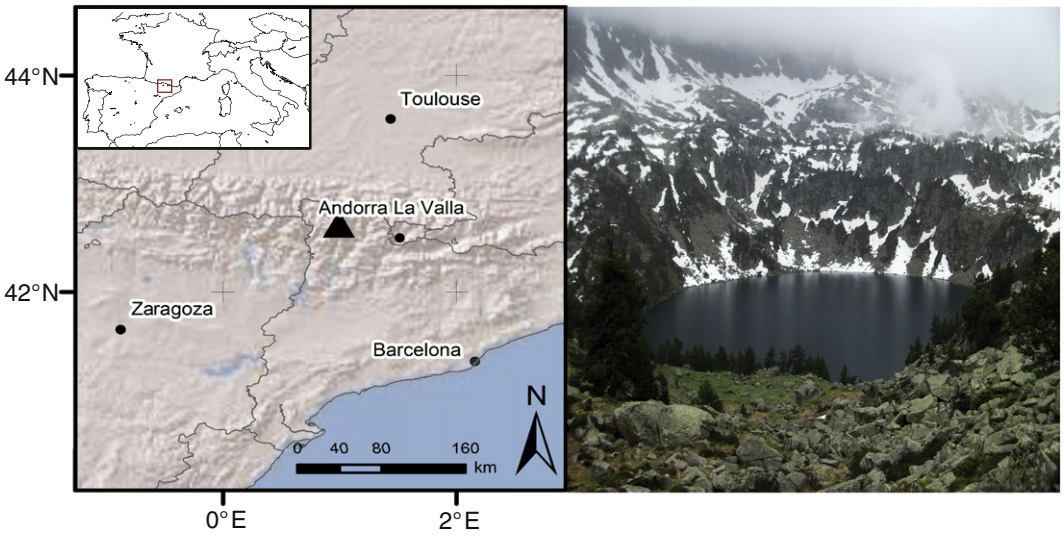

Fig. 1. *Pinus uncinata* study site at lake Gerber (right) located in the Spanish Pyrenees (left, triangle).

corrections, however, nicely match the envelop of CO_2-effects in C3-plants for CO_2 concentrations from 280 to 400 ppm detailed Schubert and Jahren (2012). The so-called pin-correction (McCarrol et al., 2009) was applied, but did not significantly modify the data (because of a slight upward trend in the $\delta^{13}C_{atm}$ data) and therefore is not discussed further. We high- and low-pass filtered the $\delta^{13}C_{atm}$, $\delta^{13}C_K$, and $\delta^{13}C_{FE}$ time series by using 20-year cubic smoothing splines for the assessment of coherence among tree-ring parameters.

2.4. Meteorological data and climate signal detection

All tree-ring time series, TRW, $\delta^{18}O$, $\delta^{13}C_{atm}$, $\delta^{13}C_K$, and $\delta^{13}C_{FE}$, were correlated against monthly temperature, precipitation, and Palmer Drought Severity Index (PDSI) data. We used temperature readings from the *Pic du Midi* mountain observatory (2862 m, 43°04′N, 0°09′E), gridded precipitation totals from the Climate Research Unit (TS 3.1; Mitchell and Jones, 2005), and gridded PDSI data from the University Corporation for Atmospheric Research (Dai et al., 2004). In addition to this widely applied drought index, we also considered a self-calibrated PDSI dataset (scPDSI), which according to van der Schrier et al. (2006) provides a more realistic estimation of the occurrence of extremes at a higher spatial resolution. When computing correlation coefficients between proxy and instrumental target data, we adjusted the degrees of freedom considering the varying autocorrelations inherent to the time series by using:

$$DF = {}^{N}\Big/\frac{1 + a1 * a2}{1 - a1 * a2}$$

with N representing the number of values (time series length), a1 the autocorrelation of series 1 (proxy data) at lag 1, and a2 the autocorrelation of series 2 (target data) at lag 1.

3. Results

3.1. Carbon isotope ratios

The $\delta^{13}C_{raw}$ measurement series include an offset of 2.24‰ (mean values range from −24.02‰ to −21.78‰) and display a decreasing trend over the 20th century visible in all five samples (Fig. 2). This decline is related to the non-climatic $\delta^{13}C$ trend in atmospheric CO_2 and removed in the $\delta^{13}C_{atm}$ data (Fig. 3). The $\delta^{13}C_K$ and $\delta^{13}C_{FE}$ chronologies, considering additional effects of the increasing CO_2 concentration on the tree's metabolism, show overall increasing trends towards present. The strongest such trend is retained in the $\delta^{13}C_{FE}$ data as a result of potentially severe influences on the carbon isotope fractionation during photosynthetic uptake.

The estimation of climate signals considers all three $\delta^{13}C$ datasets ($\delta^{13}C_{atm}$, $\delta^{13}C_K$ and $\delta^{13}C_{FE}$), thereby emphasizing potential differences due to the correction procedures (Fig. 4). $\delta^{13}C$ climatic signals are most distinct during the summer season, with the June–August season (JJA) displaying the highest positive correlation ($p < 0.001$) for temperature, and negative correlation for precipitation. The maximum seasonal response to drought varies from July–September (JAS) for PDSI, to August–September (AS) for scPDSI. The differences between these various seasons appear rather small, and can perhaps be summarized as a broader summer season signal. Highest correlations are found between summer temperature and $\delta^{13}C_{FE}$ ($r = 0.57$), followed by $\delta^{13}C_K$ ($r = 0.50$) and $\delta^{13}C_{atm}$ ($r = 0.39$). While the same order from stronger to weaker correlations ($\delta^{13}C_{FE} > \delta^{13}C_K > \delta^{13}C_{atm}$) is obtained when calibrating against PDSI, this pattern changes when calibrating against summer precipitation: $\delta^{13}C_{atm}$ ($r = -0.50$), followed by $\delta^{13}C_K$ ($r = -0.45$) and $\delta^{13}C_{FE}$ ($r = -0.34$).

These results are supported by the southern European correlation fields indicating close associations with the western Mediterranean coastal areas, from Italy to France, Spain and Northern Africa, during the summer months. Calibration against previous year instrumental data revealed more heterogeneous and less strong correlations. Previous

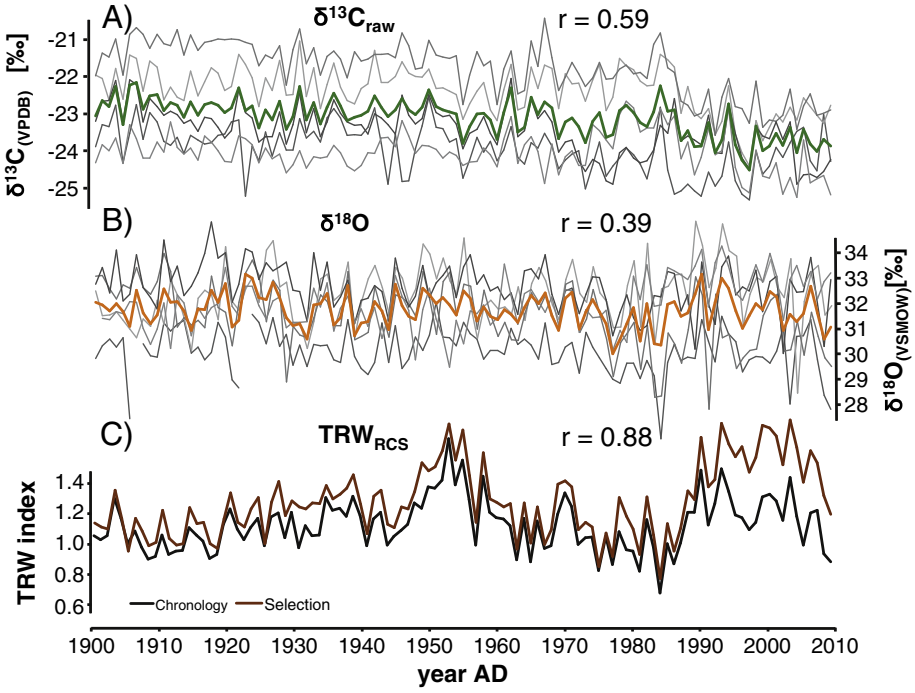

Fig. 2. Stable isotope and ring width data. (A) Uncorrected $\delta^{13}C_{raw}$ measurement series (gray) and their mean (green). (B) $\delta^{18}O$ measurement series (gray) and mean (orange), and (C) detrended TRW_{RCS} chronology (black) and selection for isotopic measurements (brown). r-values are the interseries correlations. (For interpretation of the references to color in this figure legend, the reader is referred to the web version of this article.)

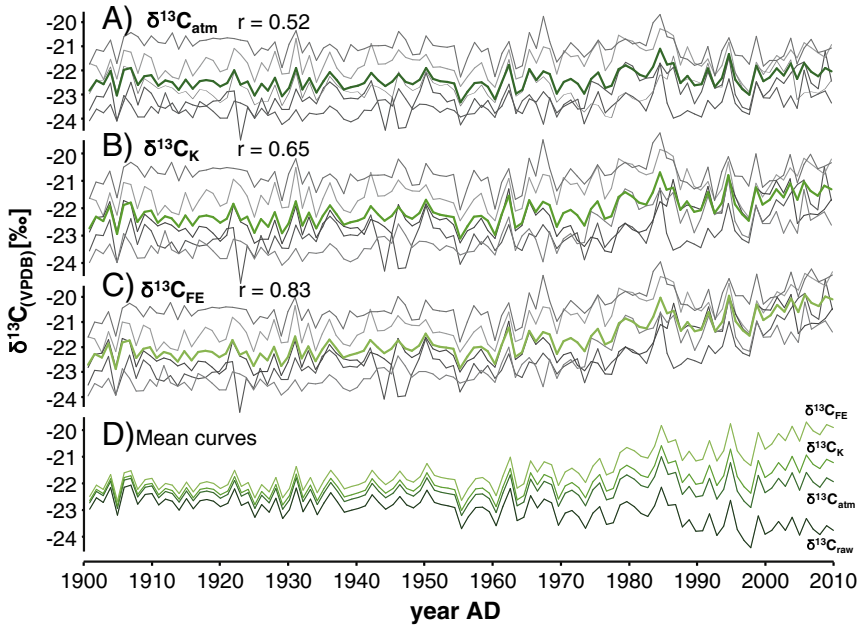

Fig. 3. Carbon isotope corrections. Single $\delta^{13}C$ time series (gray) and their means (green) after correction for decreasing values due to fossil fuel burning (A: $\delta^{13}C_{raw}$), additional correction following Kürschner (1996) (B: $\delta^{13}C_K$), and Feng and Epstein (1995) (C: $\delta^{13}C_{FE}$). (D) shows the mean curves of all carbon isotopic ratios. (For interpretation of the references to color in this figure legend, the reader is referred to the web version of this article.)

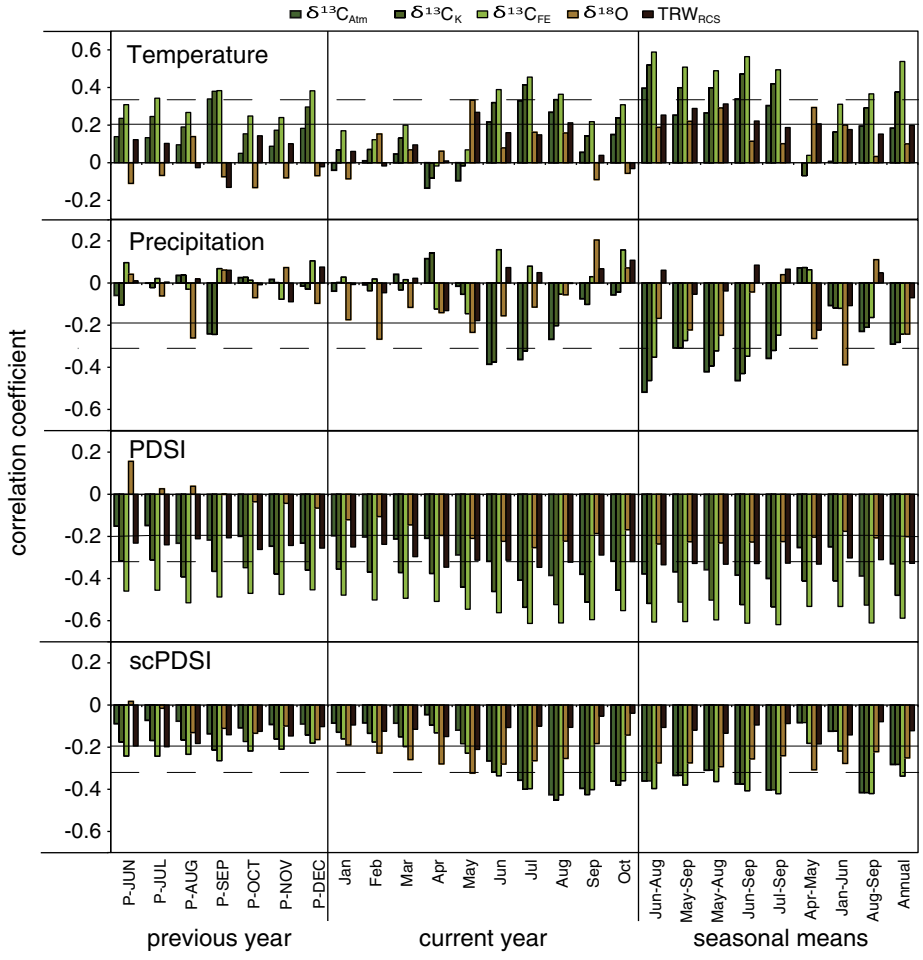

Fig. 4. Climate–isotope relationships of $\delta^{13}C$ (green: $\delta^{13}C_{atm}$, $\delta^{13}C_{CK}$, $\delta^{13}C_{FE}$), $\delta^{18}O$ (orange) and TRW_{RCS} chronologies (black) with instrumental temperature, precipitation, PDSI, scPDSI data. Correlations are computed over the period 1901–2009 (except scPDSI: 1901–2004) considering previous year June to December (left), current year January to October (middle), and current year seasonal means (right). Horizontal black lines indicate 95% significance levels and dashed lines 99.9% significance levels. Significance levels are calculated without consideration of reductions of degrees of freedom. (For interpretation of the references to color in this figure legend, the reader is referred to the web version of this article.)

year precipitation correlates significantly only during September with $\delta^{13}C_{atm}$ and $\delta^{13}C_K$. Previous year temperature, scPDSI and particularly PDSI, all show significant correlations during various months and seasons (Fig. 4), thereby indicating possibly associated autocorrelation and low-frequency trends inherent to the data, presumably caused by storage of assimilates during the winter seasons and incorporation into subsequent rings.

The correlations with target climate data increase when shortening the calibration period (starting at 1941, Fig. 6), a feature related with the sparser and less reliable early 20th century meteorological network (Wijngaard et al., 2003). We here focus on the relationship with temperature and precipitation, since the incorporation of soil moisture in the drought indices leads to high autocorrelations, causing severe reductions of degrees of freedom. Highest correlation is found between temperature and $\delta^{13}C_{FE}$ ($r = 0.63$), since both time series include similar low-frequency variations ($\delta^{13}C_{FE} > \delta^{13}C_K > \delta^{13}C_{atm}$). Although both the proxy and instrumental time series include fairly high autocorrelations (0.38 in temperature and 0.75 in $\delta^{13}C_{FE}$, at lag-1), the values remain significant ($p < 0.001$) after reduction of the degrees of freedom for serial correlation effects. The absence of low-frequency trends in $\delta^{13}C_{atm}$ leads to lower but still significant values ($p < 0.01$) when correlated with temperature. In contrast, since the precipitation data are effectively free of low-frequency trends (lag-1 autocorrelation is 0.09), $\delta^{13}C_{atm}$ shows the strongest coherence ($r = -0.64$, $p < 0.001$).

3.2. Oxygen isotope ratios

The $\delta^{18}O$ mean values of the individual time series range by 2.52‰, from 30.12‰ to 32.65‰, which is even exceeding the offset recorded in $\delta^{13}C_{raw}$. Also the variance is higher (sd = 0.65 compared sd = 0.39) indicating the influence of fluctuating source water isotopic compositions together with fractionation processes at the leaf level.

The season of strongest response to temperature and precipitation is shifted towards spring (Fig. 4), a finding deviating from the commonly reported JJA signal in European tree sites (Treydte et al., 2007; Saurer et al., 2008). Particularly the climatic conditions in May appear influential, reaching $r = 0.33$ for temperature and $r = -0.24$ for precipitation. The season from January to June displays the strongest negative correlation with precipitation ($r = -0.39$). Except for the earliest months of the year, the association between $\delta^{18}O$ and climate is generally weaker compared to $\delta^{13}C$, a finding supported by the spatial correlation patterns over the Mediterranean area (Fig. 5).

The reduced calibration period 1941–2009 (Fig. 6) exhibits a strengthened correlation with temperature ($r = 0.43$, $p < 0.001$), only slightly larger than the relationship with precipitation ($r = -0.35$, $p < 0.01$). Autocorrelation is overall lower (0.21 at lag-1) compared to the $\delta^{13}C$ data, and it is clearly evident that high temperature and low precipitation result in increased $\delta^{18}O$ values. A spring–summer drought signal is recorded in both the monthly correlations (Fig. 4) and spatial fields (Fig. 5).

4. Discussion

4.1. Carbon isotope ratios

Comparison with regional instrumental data revealed that all investigated climate parameters display higher coherences with $\delta^{13}C$ than with TRW (e.g. Büntgen et al., 2008; Dorado-Liñán et al., 2011b). These results were achieved, even though the Expressed Population Signal (EPS; Wigley et al., 1984; see Fig. S1) is higher and more stable in TRW than in the isotope datasets. The main climate signal reflected in the TRW can be attributed to water availability, here expressed as PDSI ($r = 0.34$, 1901–2009 period).

The positive correlation with summer temperature and negative correlation with precipitation revealed for $\delta^{13}C$ support previous findings based on fewer data and other species (Treydte et al., 2007; Andreu et al., 2008; Saurer et al., 2008; Dorado-Liñán et al., 2011b), and theoretical background (Helle and Schleser, 2004; Schollän et al., 2013b). The timing of cell formation is influenced by several intrinsic factors including gene expression (Schrader et al., 2004) and hormonal signals (Schrader et al., 2003), as well as environmental factors. While in the Mediterranean area cambial activity is temporally less constrained and frequently even characterized “double-stress” during summer and winter (Cherubini et al., 2003), xylem formation in our high elevation site takes place during the warm and snow-free season including all summer months. Although greenhouse studies indicated negative temperature

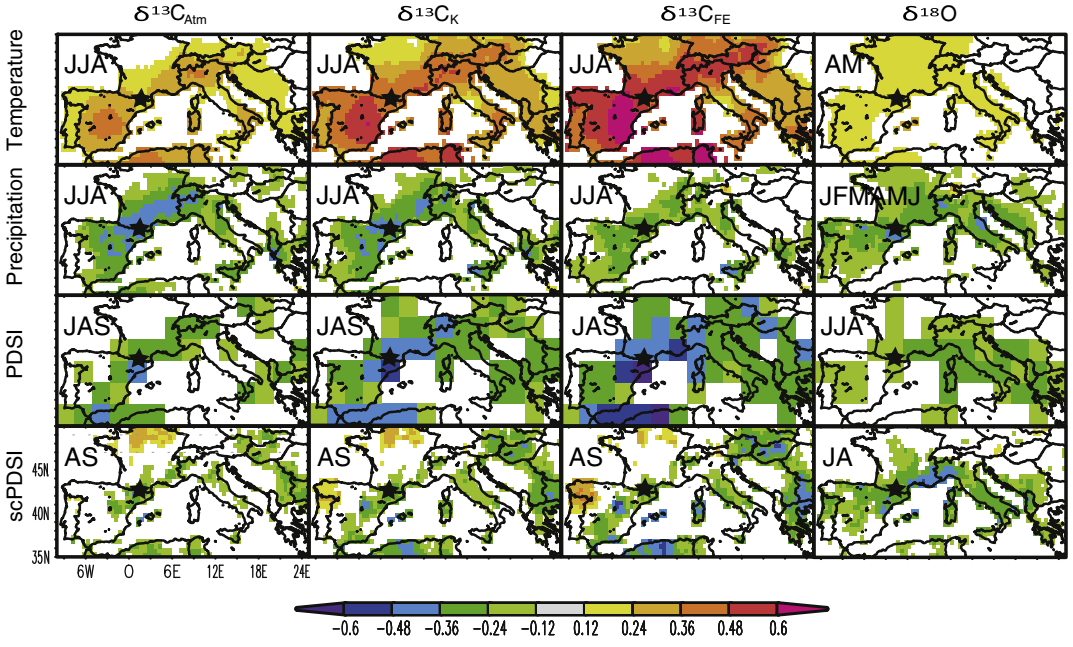

Fig. 5. Spatial field correlations between $\delta^{13}C$ and $\delta^{18}O$ chronologies and best-fit climate variables. Columns from left to right: $\delta^{13}C_{atm}$, $\delta^{13}C_K$, $\delta^{13}C_{FE}$, $\delta^{18}O$. Rows: CRUTEM 3 temperature, CRU TS 3.1 precipitation, PDSI, and scPDSI. Maps are computed using the KNMI climate explorer at http://climexp.knmi.nl. Colored areas are significant at $p < 0.10$. The sampling site is marked with a black star. (For interpretation of the references to color in this figure legend, the reader is referred to the web version of this article.)

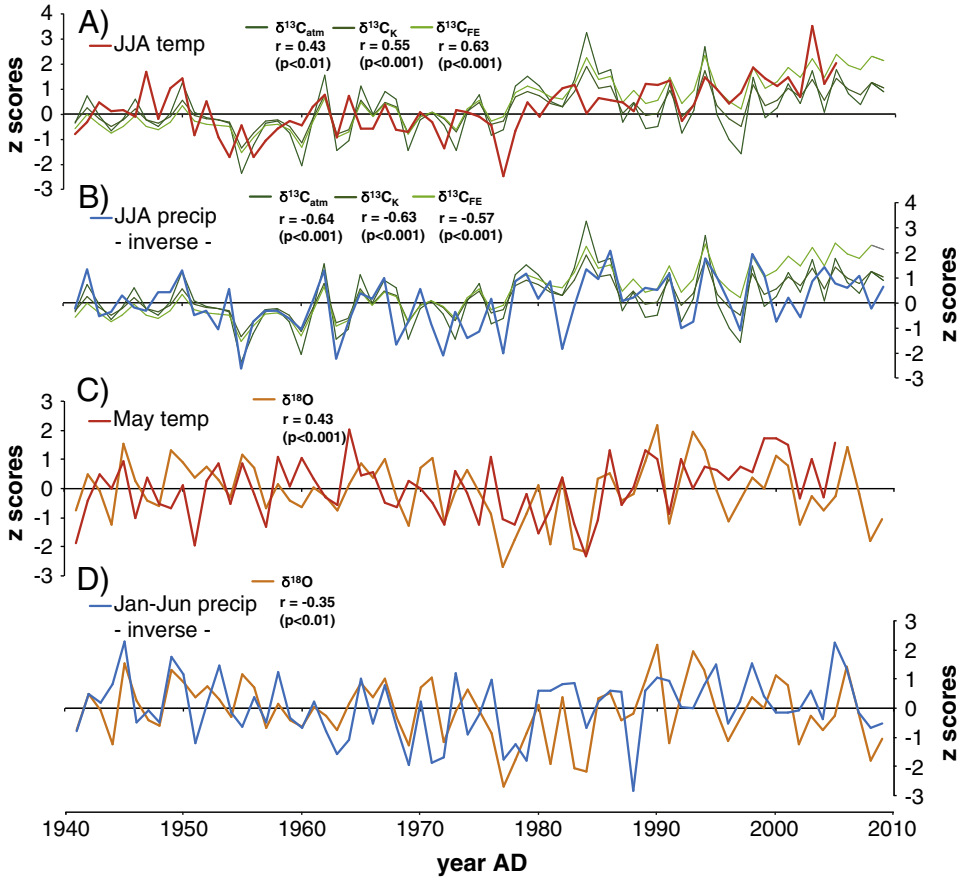

Fig. 6. Common period climate signals. (A) $\delta^{13}C$ (green) and JJA temperature (red), (B) $\delta^{13}C$ (green) and JJA precipitation (blue), (C) $\delta^{18}O$ (orange) and May temperature (red), and (D) $\delta^{18}O$ (orange) and Jan–Jun precipitation (blue). (For interpretation of the references to color in this figure legend, the reader is referred to the web version of this article.)

coefficients (Schleser et al., 1999), the higher temperatures recorded in natural environments result in positive correlations. Particularly in the Mediterranean, high temperatures are usually accompanied with high vapor-pressure deficits, and the resulting stomatal closure therefore leads to an enrichment of ^{13}C and increasing $\delta^{13}C$ (Linares et al., 2009). In contrast, precipitation events lead to reduced water vapor pressure deficits between the needles and ambient air, enabling trees to open their stomata more widely. The lower temperatures, typically accompanying summer season rain events, result in additionally reduced CO_2 assimilation rates.

As a consequence, increased leaf-internal CO_2 concentrations and depleted ^{13}C of assimilates drive the significant negative correlations between tree-ring $\delta^{13}C$ and moisture conditions during boreal summer. As summer temperature and precipitation are anti-correlated, both elements show a strong and distinct coherence with $\delta^{13}C$, though separation of these two factors remains challenging (Schleser et al., 1999; Edwards et al., 2000). This dilemma might best be compensated by considering the drought indices, PDSI and scPDSI, integrating temperature and precipitation (and soil water capacity).

To account for the Suess effect, McCarroll and Loader (2004) proposed a simple correction method, using the residuals of annually resolved $\delta^{13}C$ values of CO_2, and applying these differences to the tree-ring $\delta^{13}C_{raw}$ data (Fig. 3). As a consequence, the interseries correlation of the corrected $\delta^{13}C_{atm}$ data drops from $r = 0.59$ to $r = 0.52$, due to the removal of the common, decreasing low-frequency trend in the single measurement series. The correction procedures accounting for increasing atmospheric CO_2 concentrations ($\delta^{13}C_K$ and $\delta^{13}C_{FE}$) add additional low-frequency trend to the data, and, consequently, between-tree correlation values increase from $r = 0.65$ for $\delta^{13}C_K$ to $r = 0.83$ for $\delta^{13}C_{FE}$.

To date the procedure of correcting trends in tree-ring δ^{13} is a matter of debate within the isotope community, and there is no consensus on which of the methods reflect the fractionation processes within trees most effectively (Treydte et al., 2001, 2007; Saurer et al., 2008; Schubert and Jahren, 2012). Our results show that the varying low-frequency trends added to the data not only alter the interseries correlation among trees, but also affect the correlations between carbon isotope records and climate variables. The derived correlation patterns ($\delta^{13}C_{FE} > \delta^{13}C_K > \delta^{13}C_{atm}$) suggest a relatively strong CO_2 effect on trees growing high elevation sites in the Spanish Pyrenees.

The varying correction procedures are also reflected in changing lag-1 autocorrelations, increasing from 0.27 in $\delta^{13}C_{atm}$ to 0.49 in $\delta^{13}C_K$ and 0.76 in $\delta^{13}C_{FE}$, and in line with the 20th century temperature trend recorded in the study region (Fig. 6). The seemingly negative effects of increased autocorrelations on the degrees of freedom, when associating proxy with temperature data, make a clear distinction of the most appropriate correction procedure challenging.

The offset between individual $\delta^{13}C$ tree-ring series remains unaltered by the correction procedures, since each tree is treated equally. The substantial offset among trees (>2‰) is largely persistent throughout the 20th century. The high interseries correlation among the individual trees ($\delta^{13}C_{raw} = 0.59$) and the coherent growing conditions suggest that potentially varying climate signals cannot account for the recorded $\delta^{13}C$ offset among trees. The offset is rather caused by genetic differences in water-use efficiency and/or differing soil properties and rooting depths at the micro-site scale. The offset reported here also reinforces the importance of developing individual instead of pooling proxy series, as well as considering detrending techniques (Treydte et al., 2009; Esper et al., 2010; Dorado-Liñán et al., 2011a; Schollän et al., 2013b).

4.2. Oxygen isotope ratios

The oxygen isotopic composition in tree-rings is controlled by the isotopic composition of the water taken up via the roots, originating from precipitation in sites with no access to ground water, as well as the subsequent enrichment processes and biochemical fractionations in the needles and stem (Roden et al., 2000; Saurer et al., 2008). While the composition of meteoric H_2O is mainly driven by temperature in the Mediterranean region (Rozanski et al., 1993), leaf water enrichment is controlled by air humidity, and it is therefore expected that tree-ring $\delta^{18}O$ reflects a combination of these influences. A fraction of the leaf water enrichment is lost again when sucrose, transported from the needles to the stem, is broken up into trioses during cellulose formation and exchange of oxygen with xylem water (Roden et al., 2000). Based on these processes, positive correlations to temperatures and negative correlations air humidity, precipitation, and drought are expected, and were indeed observed in this study. In the absence of distinct low-frequency trends in the $\delta^{18}O$ time series, highest correlations were found with May temperature and Jan–Jun precipitation.

Accordingly, the climatic conditions during spring and early summer appear to be a key for the oxygen isotopic composition at the study site. Winter temperatures in our treeline site are persistently below 0 °C. Precipitation during this season generally falls as snow, while temperatures in May often exceed 0 °C providing liquid water from snow melts. These conditions can cause an apparent lag between the months of greatest influence on $\delta^{18}O$, and the months when tree growth occurs (Ehleringer and Dawson, 1992; Holzkämper et al., 2008).

The Pyrenees receive highest precipitation totals in spring, while the subsequent months are dryer. Consequently, the availability of liquid water at a higher temperature level enhances photosynthesis and stimulates cambial activity, resulting in the formation of primary earlywood cells (Rossi et al., 2008). Since water storage inside the stem during winter, at temperatures below 0 °C, bears the risk of cell destruction due to volume expansion of frozen water, trees in this area likely absorb as much liquid water as possible in the early spring season. Consequently, the isotopic composition of spring precipitation is of major importance for the signal incorporated in the cellulose.

Although the observed relationships are therefore reasonable, the $\delta^{18}O$ interseries correlation ($r = 0.39$) is weaker compared to $\delta^{13}C_{raw}$ ($r = 0.59$), a circumstance that could be related to the more complex operational sequences influencing tree-ring $\delta^{18}O$, including source water effects, leaf-level fractionations, and equilibrium reactions during assimilate transport (Treydte et al., 2007; Saurer et al., 2008). In addition, the mixed seasonal influences as discussed above may be a reason for lower correlations observed in the Mediterranean compared to more temperate, wetter regions.

4.3. Parameter coherency

Coherence between the two isotopic datasets is low, in contrast to results reported by Treydte et al. (2007) for a number of European forest sites. The $\delta^{13}C_{atm}$ and $\delta^{18}O$ time series are non-correlated ($r = -0.09$), and no association is recorded when high-pass filtering the data ($r = 0.02$) (Fig. 7). Using a 20-year low-pass filter, however, results in a negative though not significant correlation ($r = -0.44$) revealing that the *P. uncinata* $\delta^{13}C_{atm}$ and $\delta^{18}O$ chronologies share common variance at decadal to multi-decadal time scales.

5. Conclusions

Carbon isotope ratios from five high-elevation *P. uncinata* trees in the Pyrenees reflect a significant summer temperature signal over the 1941–2005 period. This signal enables the reconstruction of JJA temperatures over the western Mediterranean region. Correcting carbon isotope values for effects caused by increasing atmospheric CO_2 concentrations, adds low-frequency trend to the proxy data, which has an impact on estimating the climate signals. In subsequent climate reconstructions, the under/overestimation of adaptation processes within trees could lead to deceptive results. Consequently, correction methods have to be carried out with caution, since it is unclear, which procedure best reflects the natural adaptation of the treeline pines in the Spanish Pyrenees (Treydte et al., 2001; Saurer et al., 2008; Treydte et al., 2009).

The oxygen isotope fractionation in these trees is shown to be sensitive to spring precipitation and drought, indicating good potential for

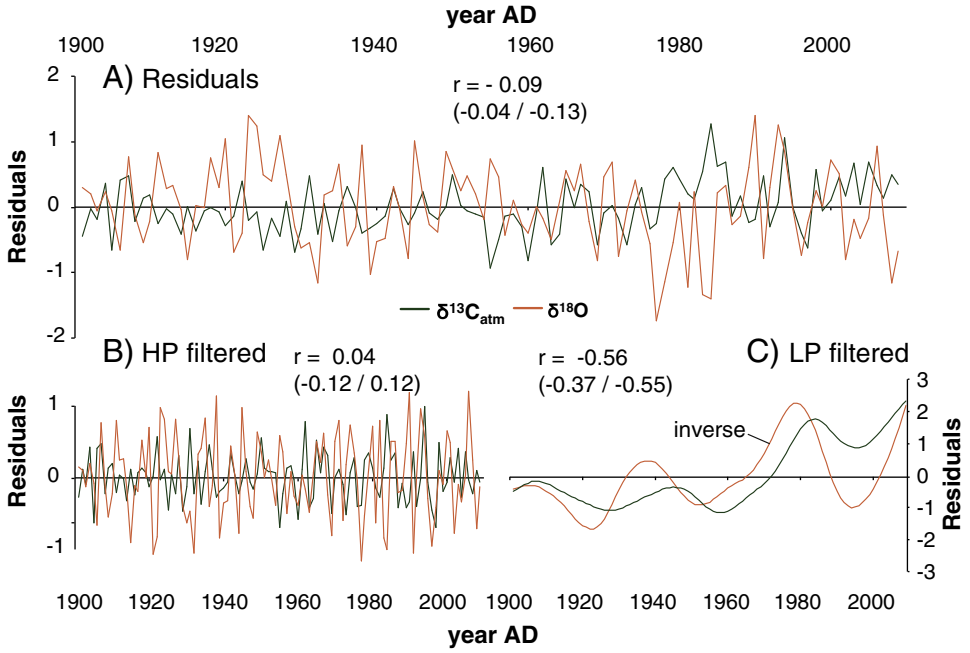

Fig. 7. Coherency between $\delta^{13}C_{atm}$ (green) and $\delta^{18}O$ (orange) over the 1901–2009 period. Correlation values in brackets refer to early (1901–1940) and late (1941–2009) calibration periods. (A) Residual time series of the 1901–2009 means. (B) High-pass filtered $\delta^{13}C_{atm}$ and $\delta^{18}O$ (residuals from 20-year cubic smoothing splines). (C) 20-year low-pass filtered $\delta^{13}C_{atm}$ and $\delta^{18}O$ time series. (For interpretation of the references to color in this figure legend, the reader is referred to the web version of this article.)

the reconstruction of hydroclimate in the Pyrenees. However, the oxygen isotope signal is not just determined by one single factor, and different seasonalities introduced by the soil water on the one hand and evaporative enrichment on the other hand, result in more complicated information encoded in this parameter (Treydte et al., 2007; Saurer et al., 2008; Dorado-Liñán et al., 2011a). Nevertheless, measurements of both $\delta^{13}C$ and $\delta^{18}O$ from *P. uncinata* in the Spanish Pyrenees offer good complementary proxy data to evaluate and reconstruct past climatic variations representative for the western Mediterranean region.

Supplementary data to this article can be found online at http://dx.doi.org/10.1016/j.chemgeo.2014.03.021.

Acknowledgments

We thank Steffen Luft for his assistance in the field, and Carmen Bürger and Heiko Baschek (supported by ICLEA, Helmholtz Association) for their laboratory support.

References

Andreu, L., Planells, O., Gutierrez, E., Helle, G., Schleser, G.H., 2008. Climatic significance of tree-ring width and $\delta^{13}C$ in a Spanish pine forest network. Tellus B 60, 771–781.
Büntgen, U., Frank, D., Grudd, H., Esper, J., 2008. Long-term summer temperature variations in the Pyrenees. Clim. Dyn. 31, 615–631.
Büntgen, U., Frank, D.C., Trouet, V., Esper, J., 2010. Diverse climate sensitivity of Mediterranean tree-ring width and density. Trees 24, 261–273.
Büntgen, U., Tegel, W., Nicolussi, K., McCormick, M., Frank, D., Trouet, V., Kaplan, J.O., Herzig, F., Heussner, K.-U., Wanner, H., Luterbacher, J., Esper, J., 2011. European climate variability and human susceptibility over the past 2500 years. Science 331, 578–582.
Büntgen, U., Frank, D., Neuenschwander, T., Esper, J., 2012. Fading temperature sensitivity of Alpine tree growth at its Mediterranean margin and associated effects on large-scale climate reconstructions. Clim. Chang. 114, 651–666.
Camarero, J.J., Guerrero-Campo, J., Gutiérrez, E., 1998. Tree-ring growth and structure of *Pinus uncinata* and *Pinus sylvestris* in the Central Spanish Pyrenees. Arct. Alp. Res. 30, 1–10.
Cherubini, P., Gartner, B.L., Tognetti, R., Bräker, O.U., Schoch, W., Innes, J.L., 2003. Identification, measurement and interpretation of tree rings in woody species from Mediterranean climates. Biol. Rev. 78, 119–148.
Cook, E.R., 1985. A Time Series Analysis Approach to Tree-ring Standardization. Univ. of Ariz, Tucson.
Craig, H., 1957. Isotopic standards for carbon and oxygen and correction factors for mass-spectrometric 467 analysis of carbon dioxide. Geochim. Cosmochim. Acta 12, 133–149.
Dai, A., Trenberth, K.E., Qian, T., 2004. A global dataset of Palmer Drought Severity Index for 1870–2002: relationship with soil moisture and effects of surface warming. J. Hydrometeorol. 5, 1117–1130.
Dorado-Liñán, I., Gutiérrez, E., Helle, G., Heinrich, I., Andreu-Hayles, L., Planells, O., Leuenberger, M., Bürger, C., Schleser, G., 2011a. Pooled versus separate measurements of tree-ring stable isotopes. Sci. Total Environ. 409, 2244–2251.
Dorado-Liñán, I., Gutiérrez, E., Heinrich, I., Andreu-Hayles, L., Muntán, E., Campelo, F., Helle, G., 2011b. Age effects and climate response in trees: a multi-proxy tree-ring test in old-growth life stages. Eur. J. For. Res. 131, 933–944.
Edwards, T.W.D., Graf, W., Trimborn, P., Stichler, W., Lipp, J., Payer, H.D., 2000. $\delta^{13}C$ response surface resolves humidity and temperature signals in trees. Geochim. Cosmochim. Acta 64, 161–167.
Ehleringer, J.R., Dawson, T.E., 1992. Water-uptake by plants —perspectives from stable isotope composition. Plant Cell Environ. 15, 1073–1082.
Esper, J., Cook, E.R., Krusic, P.J., Peters, K., Schweingruber, F.H., 2003. Tests of the RCS method for preserving low-frequency variability in long tree-ring chronologies. Tree-Ring Res. 59, 81–98.
Esper, J., Frank, D.C., Battipaglia, G., Büntgen, U., Holert, C., Treydte, K., Siegwolf, R., Saurer, M., 2010. Low-frequency noise in $\delta^{13}C$ and $\delta^{18}O$ tree-ring data: a case study of *Pinus uncinata* in the Spanish Pyrenees. Glob. Biogeochem. Cycles 24. http://dx.doi.org/10.1029/2010GB0037772.
Esper, J., Frank, D.C., Timonen, M., Zorita, E., Wilson, R.J.S., Luterbacher, J., Holzkämper, S., Fischer, N., Wagner, S., Nievergelt, D., Büntgen, U., 2012. Orbital forcing of tree-ring data. Nat. Clim. Chang. 2, 862–866.
Farquhar, G.D., O'Leary, M.H., Berry, J.A., 1982. On the relationship between carbon isotope discrimination and the intercellular carbon dioxide concentration in leaves. Aust. J. Plant Physiol. 9, 121–137.
Feng, X., Epstein, S., 1995. Carbon isotopes of trees from arid environments and implications for reconstructing atmospheric CO_2 concentration. Geochim. Cosmochim. Acta 59, 2599–2608.
Gutiérrez, E., 1991. Climatic tree growth relationships for *Pinus uncinata* ram in the Spanish pre-Pyrenees. Acta Oecol. 12, 213–225.
Heinrich, I., Touchan, R., Dorado Liñán, I., Vos, H., Helle, G., 2013. Winter-to-spring temperature dynamics in Turkey derived from tree rings since AD 1125. Clim. Dyn. http://dx.doi.org/10.1007/s00382-013-1702-3.
Helle, G., Schleser, G.H., 2004. Interpreting climate proxies from tree rings. In: Fischer, H., Floeser, G., Kumke, T., Lohmann, G., Miller, H., Negendank, J.F.W., von Storch, H. (Eds.), The Climate in Historical Times, Towards a Synthesis of Holocene Proxy Data and Climate Models. Berlin, pp. 129–148.
Holmes, R.L., 1983. Computer-assisted quality control in tree-ring dating and measurement. Tree-Ring Bull. 43, 69–78.
Holzkämper, S., Kuhry, P., Kultti, S., Gunnarson, B., Sonninen, E., 2008. Stable isotopes in tree rings as proxies for winter precipitation changes in the Russian Arctic over the past 150 years. Geochronometria 32, 37–46.
Kürschner, K., 1996. Leaf stomata as biosensors of paleoatmospheric CO_2 levels. (PhD Thesis) LPP Contributions Series No.5Utrecht University (153 pp.).
Konter, O., Holzkämper, S., Helle, G., Büntgen, U., Esper, J., 2013. Trends and signals in decadally resolved carbon isotopes from the Spanish Pyrenees. In: Helle, G., et al. (Eds.), TRACE Tree Rings in Archaeology, Climatology and Ecology. Deutsches GeoForschungsZentrum GFZ, Potsdam, Scientific Technical Report STR13/05, vol. 11. http://dx.doi.org/10.2312/GFZ.b103-13058.
Laumer, W., Andreu, L., Helle, G., Schleser, G.H., Wieloch, T., Wissel, H., 2009. A novel approach for the homogenization of cellulose to use micro-amounts for stable isotope analyses. Rapid Commun. Mass Spectrom. 23, 1934–1940.
Leavitt, S.W., Long, A., 1984. Sampling strategy for stable isotope analysis of tree rings in pine. Nature 311, 145–147.
Linares, J.-C., Delgado-Huertas, A., Camarero, J., Merino, J., Carreira, J.A., 2009. Competition and drought limit the response of water-use efficiency to rising atmospheric carbon dioxide in the Mediterranean fir *Abies pinsapo*. Oecologia 161, 611–624.
McCarroll, D., Loader, N.J., 2004. Stable isotopes in tree rings. Quat. Sci. Rev. 23, 771–801.
McCarrol, D., Gagen, M., Loader, N., Robertson, I., Anchukaitis, K., Los, L., Young, G., Jalkanen, R., Kirchhefer, A., Waterhouse, J., 2009. Correction of tree ring stable carbon isotope chronologies for changes in the carbon dioxide content of the atmosphere. Geochim. Cosmochim. Acta 73, 1539–1547.
Mitchell, T.D., Jones, P.D., 2005. An improved method of constructing a database of monthly climate observations and associated high-resolution grids. Int. J. Climatol. 25, 693–712.
Planells, O., Gutiérrez, E., Helle, G., Schleser, G.H., 2009. A forced response to twentieth century climate conditions of two Spanish forests inferred from widths and stable isotopes of tree rings. Clim. Chang. 97, 229–252.
Rinn, F., 2007. TSAP - WinTM Professional. Zeitreihenanalyse und Präsentation für Dendrochronologie und verwandte Anwendungen. Benutzerhandbuch, Heidelberg.
Roden, J.S., Lin, G.G., Ehleringer, J.R., 2000. A mechanistic model for interpretation of hydrogen and oxygen isotope ratios in tree-ring cellulose. Geochim. Cosmochim. Acta 64, 21–35.
Rossi, S., Deslauriers, A., Anfodillo, T., Carrer, M., 2008. Age-dependent xylogenesis in timberline conifers. New Phytol. 177, 199–208.
Rozanski, K., Araguas-Araguas, L., Gonfiantini, R., 1993. Isotopic patterns in modern global precipitation. In: Swart, P.K., Lohmann, K.C., McKenzie, J.A., Savin, S. (Eds.), Climate change in continental isotopic records. Washington D.C. , pp. 1–36.
Saurer, M., Cherubini, P., Reynolds-Henne, C.E., Treydte, K.S., Anderson, W.T., Siegwolf, R.T.W., 2008. An investigation of the common signal in tree ring stable isotope chronologies at temperate sites. J. Geophys. Res. 113. http://dx.doi.org/10.1029/2008JG000689.
Schleser, G.H., Helle, G., Lücke, A., Vos, H., 1999. Isotope signals as climate proxies: the role of transfer functions in the study of terrestrial archives. Quat. Sci. Rev. 18, 927–943.
Schollän, K., Heinrich, I., Neuwirth, B., Krusic, P.J., D'Arrigo, R.D., Karyanto, O., Helle, G., 2013a. Multiple tree-ring chronologies (ring width, $\delta^{13}C$ and $\delta^{18}O$) reveal dry and rainy season signals of rainfall in Indonesia. Quat. Sci. Rev. 73, 170–181.
Schollän, K., Heinrich, I., Helle, G., 2013b. UV-laser-based microscopic dissection of tree rings — a novel sampling tool for $\delta^{13}C$ and $\delta^{18}O$ studies. New Phytol. http://dx.doi.org/10.1111/nph.12587.
Schrader, J., Baba, K., May, S.T., Palme, K., Bennet, M., Bhalerao, R.P., Sandberg, G., 2003. Poplar auxin transport in the wood-forming tissues of hybrid aspen is under simultaneous control of developmental and environmental signals. PNAS 130, 10096–10101.
Schrader, J., Moyle, R., Bhalerao, R., Hertzberg, M., Lundeberg, J., Nilsson, P., Bhalerao, R.P., 2004. Cambial meristem dormancy in trees involves extensive remodelling of the transcriptome. Plant J. 40, 173–187.
Schubert, B.A., Jahren, A.H., 2012. The effect of atmospheric CO_2 concentration on carbon isotope fractionation in C3 land plants. Geochim. Cosmochim. Acta 96, 29–43.
Tardif, J., Camarero, J.J., Ribas, M., Gutiérrez, E., 2003. Spatiotemporal variability in tree growth in the Central Pyrenees: climatic and site influences. Ecol. Monogr. 73, 241–257.
Treydte, K., Schleser, G.H., Schweingruber, F.H., Winiger, M., 2001. The climatic significance of $\delta^{13}C$ in subalpine spruces (Lötschental, Swiss Alps): a case study with respect to altitude, exposure and soil moisture. Tellus B 53, 593–611.
Treydte, K., et al., 2007. Signal strength and climate calibration of a European tree ring isotope network. Geophys. Res. Lett. 34. http://dx.doi.org/10.1029/2007GL031106.
Treydte, K., Frank, D.C., Saurer, M., Helle, G., Schleser, G.H., Esper, J., 2009. Impact of climate and CO_2 on a millennium-long tree-ring carbon isotope record. Geochim. Cosmochim. Acta 71, 4635–4647.
Van der Schrier, G., Briffa, K.R., Jones, P.D., Osborn, T.J., 2006. Summer moisture variability across Europe. J. Clim. 19, 2818–2834.
Wieloch, T., Helle, G., Heinrich, I., Voigt, M., Schyma, P., 2011. A novel device for batch-wise isolation of α-cellulose from small-amount wholewood samples. Dendrochronologia 29, 115–117.
Wigley, T.M.L., Briffa, K.R., Jones, P.D., 1984. On the average value of correlated time series, with applications in dendroclimatology and hydrometerology. J. Clim. Appl. Meteorol. 23, 201–213.
Wijngaard, J.B., Klein Tank, A.M.G., Können, G.P., 2003. Homogeneity of 20th century European daily temperature and precipitation series. Int. J. Climatol. 23, 679–692.